

# Luminescence blinking of a Si quantum dot in a SiO<sub>2</sub> shell

Ilya Sychugov, Robert Juhasz, and Jan Linnros

*Laboratory of Materials and Semiconductor Physics, Royal Institute of Technology, SE-16440, Kista-Stockholm, Sweden*

Jan Valenta

*Faculty of Mathematics and Physics, Department of Chemical Physics and Optics, Charles University, Ke Karlovu 3, Prague 2, CZ-12116, Czech Republic*

(Received 13 December 2004; published 29 March 2005)

The phenomenon of on-off luminescence intermittency—blinking—in silicon nanocrystals was studied using a single-dot microphotoluminescence technique. From recordings of the luminescence intensity trace, on- and off-time distributions were extracted revealing exponential behavior, as expected for systems with blinking of a purely random nature. The corresponding switching rates for on-off and off-on processes exhibit different dependence on the excitation intensity. While the on-off switching rate grows quadratically with the excitation, the inverse process is nearly pumping power independent. Experimental findings are interpreted in terms of a dot “charging” model, where a carrier may become trapped in the surrounding matrix due to thermal and Auger-assisted processes. Observed blinking kinetics appear to be different from that of porous silicon particles.

DOI: 10.1103/PhysRevB.71.115331

PACS number(s): 78.55.Ap, 78.67.Hc

## I. INTRODUCTION

Optical properties of semiconductor nanocrystals are largely dependent on surface properties as well as on the surrounding matrix. One example is exciton scattering with interface states, which may impose limitations on coherence times in quantum dots (QDs), leading to the experimental observations of relatively broad homogeneous linewidths even at cryogenic temperatures.<sup>1</sup> Another manifestation of the influence of environment on real QDs is the phenomenon of luminescence on-off blinking. Such sudden interruptions of light emission from a QD have attracted much attention recently due to their complex physics and importance in nanocrystal applications. Indeed, the blinking lowers the effective quantum efficiency for a QD and thereby degrades the performance of any device built on ensembles of QDs. One of the generally accepted concepts for on-off blinking explains this effect in terms of carrier trapping in the matrix surrounding the QD, which in turn promotes Auger-assisted quenching of the luminescence; when the carrier returns back, the luminescence is restored.<sup>2</sup> It has also been shown that blinking may exhibit unique kinetics for different QDs in various matrices.<sup>3,4</sup>

Despite the long lifetime of excitons in silicon nanocrystals (usually in the range 10–100  $\mu$ s, i.e., 4–5 orders of magnitude larger than in some direct bandgap QDs), interest in them is promoted by the well-developed VLSI technology. In most cases silicon nanocrystals are produced as embedded in a SiO<sub>2</sub> matrix (e.g., by ion beam implantation of Si ions into silica and subsequent annealing).<sup>5</sup> In this case the interaction with an ambient medium also plays an important role in the optical behavior of QDs. The passivation of interface states with hydrogen in such silicon nanocrystals proved to have significant impact on their luminescent properties.<sup>6,7</sup> Also “pinning” of quantum confined states was shown for small nanocrystals by considering a Si=O bond related defect state in the bandgap.<sup>8</sup> However, no study on blinking in Si

QDs has been performed so far largely due to the extreme experimental complexity of such single-dot experiments. Although this effect was recently investigated for porous Si particles,<sup>9</sup> there are some substantial differences between these two low-dimensional entities as we show in a separate study.<sup>10</sup> Briefly, unlike true nanocrystals,<sup>11</sup> porous Si particles do not possess sharp emission lines at low temperature and their blinking statistics reveal more than two states, suggesting the existence of several luminescence chromophores within a single particle. Thus, it seems difficult to produce a single QD from porous Si particles, which still remain a complex network of nanocrystals,<sup>13</sup> despite many filtering and thinning out procedures.

Previously we showed that the procedure of nanocrystal formation by electron beam lithography, plasma etching, and subsequent size reduction by a careful oxidation scheme may result in well-resolved arrays of single Si nanocrystals.<sup>11,14</sup> Characteristic sharp linewidths at low temperatures, exciton-phonon interactions, dot-to-dot variations in the emission pattern were reported. In addition, a bandgap narrowing with increasing temperature, similar to that of bulk Si, was observed for such QDs.<sup>15</sup> Altogether, these findings are strongly indicating that the luminescence originates from single QDs.

Here we report results of blinking studies for a Si QD under different excitation conditions. The observed strong dependence of the on-off switching rate on excitation intensity suggests Auger-assisted ionization of a QD at higher excitation regimes. The exponential nature of blinking kinetics reported here differs from the power-law dependence observed for porous Si particles.

## II. EXPERIMENTAL DETAILS

Samples in the form of pillar arrays were fabricated using electron beam lithography and reactive ion etching followed by oxidation to form nanocrystals at the pillar tops.<sup>11,14</sup>

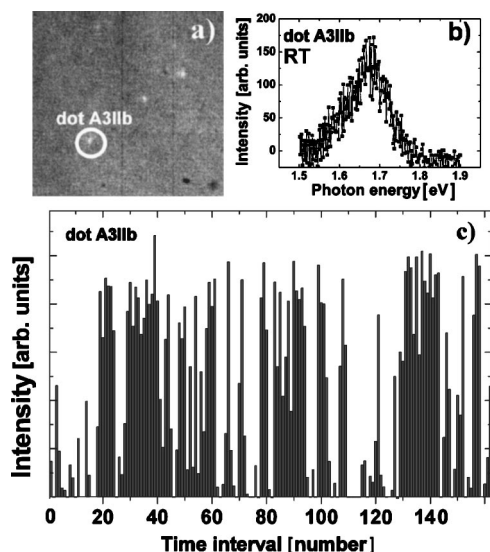


FIG. 1. (a) PL image of an array of silicon quantum dots. The dot which is analyzed in the present work is highlighted, (b) Room-temperature PL spectra of the QD (peak energy  $\sim 1.7$  eV corresponds to a  $\sim 3$ –4 nm diameter Si QD), (c) A fraction of the luminescence intensity trace for the same dot with 15 seconds integration time per interval.

N-type Si wafers with a 25 nm thermal oxide were used as substrates and holes with a diameter of  $\sim 100$  nm were defined by an electron beam in a positive type of resist. This was followed by lift off of NiCr and reactive ion etching to produce  $\sim 200$  nm tall Si pillars. Thermal oxidation at  $900^\circ\text{C}$  induced a shrinking of the Si cores of the pillars, leading to the formation of a silicon nanocrystal at the top of pillars as a result of the self-limiting oxidation, known to occur for a small radius of curvature. Low-temperature PL studies revealed different emission photon energies in the range from 1.5 to 2.0 eV for such prepared nanocrystals.<sup>11</sup> According to the quantum-confinement theory and size-separation experiments this range corresponds to Si nanocrystals, embedded into a  $\text{SiO}_2$  matrix, with sizes from 3 to 6 nm in diameter.<sup>12</sup> Variations in the emission pattern observed by spectroscopy characterization were ascribed to variations in dots size, geometry, and strain.

Room temperature PL was excited by the UV line (325 nm) of a cw He-Cd laser with variable pumping intensity. The light emitted from a sample was collected by a high-magnification objective with a large numerical aperture ( $\text{NA}=0.7$ ). An imaging spectrometer coupled to a liquid nitrogen cooled charge coupled device (CCD) camera was employed to detect the luminescence. A PL image of pillar arrays is shown in Fig. 1(a). Although most luminescent dots were characterized by on-off blinking with dominant off state, we selected a dot with comparable average on and off time. This choice makes more convenient the tracking of changes in on and off times under variable excitation. The selected dot is indicated by a circle in Fig. 1(a).

### III. RESULTS

A typical luminescence intensity trace from a Si QD is shown in Fig. 1(c). The most straightforward way of blinking

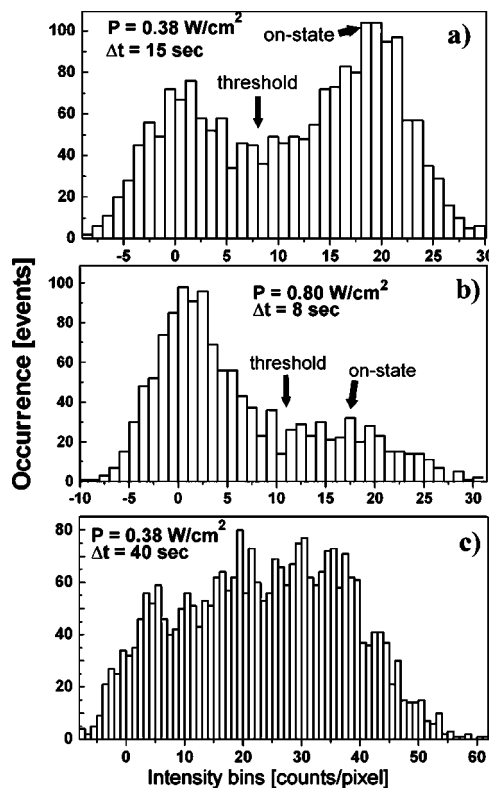


FIG. 2. Statistics of the intensity trace under various experimental conditions. (a), (b) Luminescence intermittence between two states (on and off) is clearly visible for the same QD under different pumping regimes. Peaks are broadened due to the noise contribution. (c) Long acquisition time per interval (40 s) smears off the two-level structure of the trace. Compare to (a) where a shorter time interval (15 s) was chosen under the same experimental conditions.

data processing is based on a pre-estimated threshold value, separating on and off states.<sup>16</sup> In order to corroborate the fact that intensity intermittence takes place between only two states (on and off) we calculated the frequency with which certain intensity values occur in the trace. Ideally, such statistical breakdown of the intensity time dependence would yield two  $\delta$  functions, corresponding to each state. In practice, the chosen time resolution and the CCD read-out noise transform  $\delta$  functions into Gaussian-shaped curves, as seen in Figs. 2(a) and 2(b) (naturally, intermediate intensity values appear when switching occurs during an integration time interval). It is important to note that such statistical analysis can reveal the presence of two discrete states only if time resolution has been chosen correctly. If the chosen interval value was too long then intermediate states would enter and a statistical breakdown of the trace would not reveal any distinct on and off states at all [Fig. 2(c)]. On the other hand, the integration interval cannot be set too small due to signal-to-noise considerations. Therefore for each excitation regime the actual time resolution was chosen individually.

After a trace with a proper time resolution was recorded, a threshold value, separating on and off states, can be established [Figs. 2(a) and 2(b)]. Finally, statistics of the plateau duration for on and off states can be calculated, assuming that all data points below the threshold correspond to the off

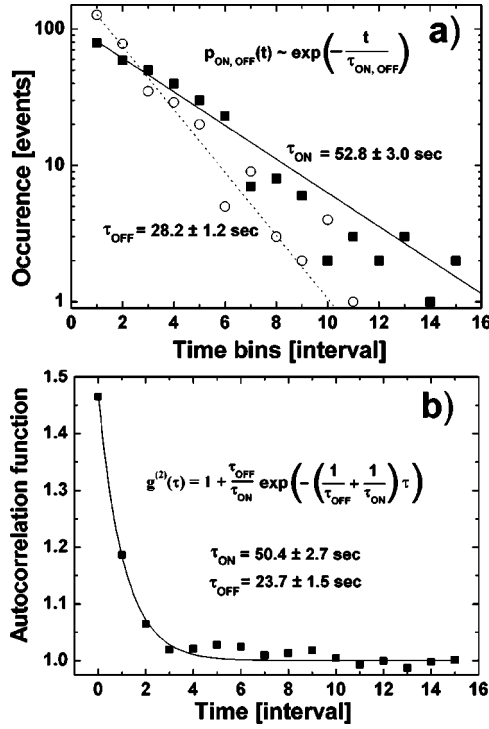


FIG. 3. The analysis of blinking data for excitation intensity  $\sim 0.38 \text{ W/cm}^2$  and the integration interval 15 s. (a) On (dark squares) and off (open circles) time distributions. Exponential dependence is seen. Characteristic times obtained from line slopes are given. (b) Data points are the values of the autocorrelation function calculated by Eq. (2) directly from the intensity trace. Solid line is a fit to the data points based on the expression (4) for the autocorrelation function in the case of a purely random on-off switching. Time constants obtained by this model are shown.

state, while the rest to the on state. In Fig. 3(a) calculated distributions are shown, where the fitting is based on a random switching model

$$p_{\text{on,off}}(t) \sim \exp\left(-\frac{t}{\tau_{\text{on,off}}}\right), \quad (1)$$

where  $\tau_{\text{on}}$  and  $\tau_{\text{off}}$  are average durations of on and off states correspondingly. It should be noted that observed blinking kinetics clearly differ from the power-law distribution found for porous Si particles.<sup>9</sup> The two possible distributions correspond to specific physical processes: an exponential distribution manifests a purely random process of switching between two states, while a power-law dependence is more deterministic, i.e., random with some inherent restrictions.

An alternative method for characterizing a random two-state process is based on a second order normalized autocorrelation function  $g^{(2)}(\tau)$ :

$$g^{(2)}(\tau) = \frac{\langle I(t) \rangle \cdot \langle I(t + \tau) \rangle}{\langle I(t) \rangle^2}. \quad (2)$$

In Ref. 16 this function was derived for the case of nonexponential on- and off-time distributions. Here, we follow the authors closely to obtain an analytical expression for this

function in the case of single-exponential distributions of plateau durations for both on and off states, as observed in the present experiment [Fig. 3(a)]. Using Laplace transforms of the normalized on- and off-time distributions one obtains

$$\tilde{g}^{(2)}(s) = \frac{(s\tau_{\text{off}} + 1)(\tau_{\text{on}} + \tau_{\text{off}})}{s(s\tau_{\text{on}}\tau_{\text{off}} + \tau_{\text{on}} + \tau_{\text{off}})}, \quad (3)$$

the inverse Laplace transform of which yields

$$g^{(2)}(\tau) = 1 + \frac{\tau_{\text{off}}}{\tau_{\text{on}}} \exp\left[-\left(\frac{1}{\tau_{\text{on}}} + \frac{1}{\tau_{\text{off}}}\right)\tau\right]. \quad (4)$$

In Fig. 3(b) autocorrelation function data points, calculated directly from the trace using expression (2), are shown. We fit these data with a function in the form of Eq. (4) with  $\tau_{\text{on}}$  and  $\tau_{\text{off}}$  as fitting parameters (solid line). It is seen that the values for average times in on and off states obtained by this method are similar to those calculated by the previously discussed threshold approach [see Fig. 3(a)].

In order to track changes in the blinking process with increasing excitation it is more convenient to use the switching rate for on-off and off-on events rather than the average time in a certain state. Using single-exponential distributions one can define switching rates as

$$f_{10,01} \equiv \frac{\sum_{n=1}^{\infty} \exp(-n/\tau_{\text{on,off}})}{\sum_{n=1}^{\infty} \exp(-n/\tau_{\text{on,off}})n} \frac{1}{\Delta t} \approx \left[1 - \exp\left(-\frac{1}{\tau_{\text{on,off}}}\right)\right] \frac{1}{\Delta t}, \quad (5)$$

where  $f_{10,01}$  is the switching rate for on-off and off-on processes correspondingly (Hz),  $\tau_{\text{on,off}}$  is the average time in on and off states (number of intervals), and  $\Delta t$  is the observation interval length (sec). The numerator in this formula stands for the total number of switching events, while the denominator accounts for the overall number of time intervals spent in the corresponding state. At the limit of long average times the switching rate becomes simply the inverse of the corresponding average time:  $f_{10,01} \approx 1/(\tau_{\text{on,off}} \Delta t)$ . The latter value was used in Ref. 4 and referred to as a “characteristic switching rate.”

Switching rates, calculated from Eq. (5) for recorded luminescence intensity traces, are shown in Fig. 4 as a function of excitation power density. Corresponding average times in on and off states at various excitation regimes were found from the threshold approach analysis of the experimental data.

#### IV. DISCUSSION

As can be seen from Fig. 4, the switching rate for the on-off process is clearly dependent on the excitation intensity, while the inverse process shows rather weak dependence. In order to explain these observations we employ a model for blinking developed by Efros and Rosen.<sup>2</sup> According to this concept, after an exciton was created in a quantum dot the escape of one of the carriers to a trap site outside the

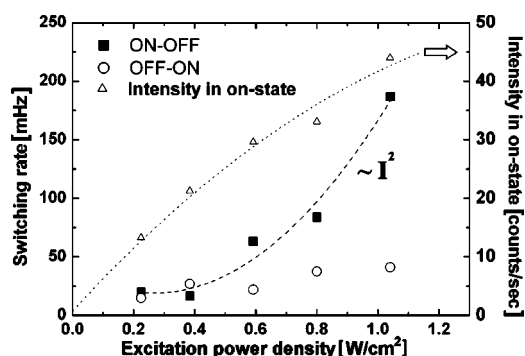


FIG. 4. Switching rates for the QD under different excitation regimes. The data for the on-off switching rate are fitted with a square dependence on excitation intensity, as discussed in the text. The luminescence intensity in the on-state is also shown as a function of excitation. A deviation from the linear regime is visible at higher excitation values. The dotted line is merely a guide for an eye.

nanocrystal makes it optically dark due to the quenching of the luminescence in the now charged quantum dot. The return of the carrier restores initial conditions. The carrier is presumably an electron rather than a hole due to the smaller effective mass of the electron. The relatively long average times in on and off states, observed in the present experiment, suggest that the traps are located in the surrounding matrix rather than on the interface.<sup>17</sup>

In general, the transfer of a carrier from a nanocrystal to a trap state can be thermally induced, Auger-assisted or occur as a result of a direct photon impact. By the latter here we mean the process of a complete energy transfer from an incident photon to a previously excited electron in the conduction band of a nanocrystal. In addition, for trap sites with an appropriate energy position a tunneling can take place, which depends on the barrier height and remoteness of the trap from the nanocrystal only. For the present experiment we rule out the possibility of direct photon impact because of relatively low excitation intensities used.<sup>2</sup> Pure tunneling should not depend on the pumping power. Unless there is a local heating of the nanocrystal induced by the incident laser beam, the contribution from temperature-induced ionization should also be excitation intensity independent. Thus, the most probable physical process responsible for the observed on-off switching rate dependence is Auger ionization. Since the probability of finding two excitons in the same quantum dot grows quadratically with increasing excitation, we fitted the data for on-off switching rate in Fig. 4 with a second order polynomial function. The fitting reproduces the main trend correctly, assuming the existence of an excitation intensity independent pedestal, which originates from one of the pumping-independent processes mentioned above. The lack of strong dependence found for the inverse process seems quite natural since Auger-induced transfer of energy is highly unlikely for a carrier localized somewhere outside the nanocrystal. However, the probability of this process may be different from zero and, generally, it could be responsible for the observed slight increase of the off-on switching rate with excitation intensity. Another possible reason is local heating at higher pumping regimes, which promotes temperature-

induced return of the carrier back to the nanocrystal. Although no change in sample temperature was detected under the laser irradiation, the fact that a NC is embedded into the material with very low thermal conductivity makes possible local heating of the QD with increasing pumping. Both on-off and off-on switching rates would be affected similarly by applying higher excitation in such a case. Thus, the observed slight increase of the switching rate for the off-on process might be also inherent to the on-off transition. Here this trend is, probably, screened by a more dramatic Auger-induced growth of the on-off switching rate.

In Fig. 4 we also plotted measured luminescence intensity in the on state as a function of excitation. Note that the deviation from the linear regime occurs at similar power densities as the on-off switching rate starts growing. The luminescence intensity bends towards saturation when it becomes exciton lifetime limited rather than pumping power limited. At this excitation regime more than one exciton can be found occasionally in a QD at a time. Thus, this fact supports the probable involvement of the Auger process in the ejection of a carrier from a nanocrystal. The presence of two excitons would normally be detected as a second “biexciton” line shifted from the normal PL line by a few meV. We were searching for this line at low-temperature measurements but did not observe it.<sup>11</sup> Therefore we conclude that the Auger process is of high probability when more than one exciton is present in a Si QD.

From the intensity data in the on state, well-below saturation, we estimated the quantum efficiency in the on state for such a quantum dot. The estimations yield the value  $\sim 15\%$ , similar to values reported previously for these nanocrystals.<sup>14</sup> It is seen in Fig. 4 that the on-off switching rate grows faster than the luminescence intensity in the on state, which rather tends to saturation with increasing excitation. These trends together lead to less light output from a QD when stronger pumping is applied.

We suppose that the role of the Auger process can be generalized to all Si quantum dots embedded in a  $\text{SiO}_2$  matrix. However, the characteristic times of blinking are individual for different nanocrystals. Moreover, the effect of changing temperature alters blinking parameters drastically for various dots. Some dots spend considerably longer time in the on state at certain temperature intervals, while others become almost dark. We ascribe these variations to the unique trap configurations for the surroundings of each dot. Although inherent defect states in bulk silica have been widely investigated (e.g., in Ref. 18), the stress from oxidation and strong curvature at the interface, common for Si nanocrystals in a  $\text{SiO}_2$  matrix, may lead to various scenarios of trap site formation for different dots.

## V. CONCLUSIONS

We have investigated the process of blinking for single silicon quantum dots embedded in a  $\text{SiO}_2$  matrix. Observed exponential blinking kinetics differ substantially from the power-law distribution of on- and off-times measured for porous silicon particles. The switching rate for the on-off process exhibits strong dependence on the excitation inten-



sity, and was ascribed to Auger-assisted ionization of a QD. The inverse, off-on process, was found to be comparatively excitation intensity independent. It appears that silicon dioxide as an ambient medium for silicon nanocrystals provides a variety of trap sites capable of capturing a charge from a QD. The individuality of trap geometry, in turn, leads to an individuality of blinking characteristic times for different single quantum dots.

# ACKNOWLEDGMENTS

We would like to thank A. Galeckas for technical assistance and D. Haviland of the KTH Nanofabrication lab for the access to the *e*-beam lithography setup. Support for this work was provided by the Swedish Research Council (V.R.). One of the authors (J.V.) acknowledges funding from the GACR (202/03/0789) and GAAV (IAA1010413) grant agencies.

- 
- <sup>1</sup>Y. Masumoto, in *Semiconductor Quantum Dots*, edited by Y. Masumoto and T. Takagahara (Springer-Verlag, Berlin, 2002), p. 346.
  - <sup>2</sup>A. L. Efros and M. Rosen, *Phys. Rev. Lett.* **78**, 1110 (1997).
  - <sup>3</sup>M. Kuno, D. P. Fromm, H. F. Hamann, A. Gallagher, and D. J. Nesbitt, *J. Chem. Phys.* **112**, 3117 (2000).
  - <sup>4</sup>M.-E. Pistol, P. Castrillo, D. Hessman, J. A. Prieto, and L. Samuelson, *Phys. Rev. B* **59**, 10 725 (1999).
  - <sup>5</sup>J. Linnros, N. Lalic, A. Galeckas, and V. Grivickas, *J. Appl. Phys.* **86**, 6128 (1999).
  - <sup>6</sup>A. R. Wilkinson and R. G. Elliman, *Phys. Rev. B* **68**, 155302 (2003).
  - <sup>7</sup>B. K. Meyer, V. Petrova-Koch, T. Muschik, H. Linke, P. Omling, and V. Lehmann, *Appl. Phys. Lett.* **63**, 14 (1993).
  - <sup>8</sup>M. V. Wolkin, J. Jorne, P. M. Fauchet, G. Allan, and C. Delerue, *Phys. Rev. Lett.* **82**, 197 (1998).
  - <sup>9</sup>F. Cichos, J. Martin, and C. von Borczyskowski, *Phys. Rev. B* **70**, 115314 (2004).
  - <sup>10</sup>J. Linnros, I. Sychugov, and J. Valenta (unpublished).
  - <sup>11</sup>I. Sychugov, R. Juhasz, J. Valenta, and J. Linnros, *Phys. Rev. Lett.* **94**, 087405 (2005).
  - <sup>12</sup>G. Ledoux, J. Gong, F. Huisken, O. Guillois, and C. Reynaud, *Appl. Phys. Lett.* **80**, 4834 (2002).
  - <sup>13</sup>A. G. Cullis, L. T. Canham, and P. D. J. Calcott, *J. Appl. Phys.* **82**, 909 (1997).
  - <sup>14</sup>J. Valenta, R. Juhasz, and J. Linnros, *Appl. Phys. Lett.* **80**, 1070 (2002).
  - <sup>15</sup>I. Sychugov, R. Juhasz, A. Galeckas, J. Valenta, and J. Linnros, *Opt. Mater. (Amsterdam, Neth.)* **27**, 973 (2005).
  - <sup>16</sup>R. Verberk, A. M. van Oijen, and M. Orrit, *Phys. Rev. B* **66**, 233202 (2002).
  - <sup>17</sup>M. Kuno, D. P. Fromm, S. T. Johnson, A. Gallagher, and D. J. Nesbitt, *Phys. Rev. B* **67**, 125304 (2003).
  - <sup>18</sup>M. Watanabe, S. Juodkasis, H.-B. Sun, S. Matsuo, and H. Misawa, *Phys. Rev. B* **60**, 9959 (1999).